# Two-Step Spin Crossover in the New Dinuclear Compound $[Fe(bt)(NCS)_2]_2bpym$, with bt = 2,2'-Bi-2-thiazoline and bpym = 2,2'-Bipyrimidine: Experimental Investigation and Theoretical Approach

**José-Antonio Real,[1a] Hélène Bolvin,[1b] Azzedine Bousseksou,[1c] Ary Dworkin,[1d] Olivier Kahn,*[,1b] François Varret,[1c] and Jacqueline Zarembowitch*[,1b]**

*Contribution from the Departamento de Química Inorganica, Universitat de València, 46100 Burjassot (València), Spain, the Laboratoire de Chimie Inorganique, URA CNRS 420, and Laboratoire de Chimie Physique des Matériaux Amorphes, URA CNRS 1104, Université Paris-Sud, 91405 Orsay, France, and Département de Recherches Physiques, URA CNRS 71, Université Pierre et Marie Curie, 75252 Paris, France.* *Received November 14, 1991*

**Abstract:** This paper is concerned with the first two-step spin crossover presented by a polynuclear molecular compound, viz., the dinuclear iron(II) complex $[Fe(bt)(NCS)_2]_2bpym$, where bt stands for 2,2'-bi-2-thiazoline and bpym for the bridging ligand 2,2'-bipyrimidine. The synthesis of the compound is described. Variable-temperature magnetic susceptibility and $^{57}Fe$ Mössbauer spectrometry data provide evidence for an overall $S = 2$ (HS) $\leftrightarrow$ S = 0 (LS) spin-crossover behavior. They show that the transition takes place in two steps. The so-called "step 1" and "step 2" are centered around 163 and 197 K, respectively. The former is more abrupt than the latter. The thermal variation of the quadrupole splitting of the HS doublet ($\Delta E_q^{HS}$) confirms that the sample is made of a single structural phase and roughly accounts for the intramolecular processes LS,LS $\leftrightarrow$ LS,HS (step 1) and LS,HS $\leftrightarrow$ HS,HS (step 2). The differential scanning calorimetry diagram exhibits two peaks, a sharp one pointing at 164 K and a broad one with a maximum at 194 K. The overall enthalpy and entropy variations are found to be $\Delta H = 13.3 \pm 0.5$ kJ mol$^{-1}$ and $\Delta S = 82 \pm 6$ J K$^{-1}$ mol$^{-1}$, respectively. The cornerstone of the theoretical approach which has been developed to account for a two-step transition in iron(II) dinuclear species is that the enthalpy $H_{SQ}$ of the mixed-spin species SQ (S = spin singlet; Q = spin quintet) is not exactly halfway between the enthalpies $H_{SS}$ and $H_{QQ}$ of the like-spin species SS and QQ, respectively. It turns out that it can be written $H_{SQ} = (H_{SS} + H_{QQ})/2 + W$. $W \neq 0$ is due to both electrostatic and vibronic effects. $W > 0$ makes the transition more abrupt; on the other hand, $W < 0$ may lead to a two-step transition. Actually, the two-step character is due to the synergistic effect of intramolecular interactions favoring SQ ($W < 0$) and intermolecular interactions favoring like-species domains (intermolecular interaction parameter $\gamma > 0$). Our model leads to quite a satisfying fitting of the magnetic data with $\Delta H = 13.16$ kJ mol$^{-1}$, $\Delta S = 73.69$ J K$^{-1}$ mol$^{-1}$, $W = -478$ J mol$^{-1}$, and $\gamma = 2.572$ kJ mol$^{-1}$. Furthermore, using those energy parameters results in a simulation of the heat capacity versus temperature curve showing the main features of the experimental curve, in particular a sharp and intense peak around 163 K and a broader and less intense peak around 197 K.

## Introduction

Most of the known thermally- or pressure-induced high-spin state (HS) $\leftrightarrow$ low-spin state (LS) crossovers presented by transition metal molecular compounds were found to take place in one step: in other words, the curve representing the variation of the metal ion HS fraction ($n_{HS}$) as a function of the external perturbation shows a unique inflexion point.[2-5]

However, a few rare examples of two-step spin conversions were also reported. Such a magnetic behavior was first described as early as 1969 in the case of the iron(III) compound $H[Fe(5\text{-}Br\text{-}thsa)_2]$, where 5-Br-thsa is a substituted salicylaldehyde thiosemicarbazone.[6,7] More recently, it was detected[8] in the iron(II) complex $[Fe(2\text{-}pic)_3Cl_2]\cdot EtOH$ (where 2-pic = 2-picolylamine), then extensively investigated,[9-15] and associated with the presumed existence of static density waves of the HS form in the range of the transition.[15] Other two-step iron(II) spin changes were afterwards described: an extended intermediate plateau of $\approx$30 K was observed in the temperature dependence of $n_{HS}$ relative to the spin-crossover system $Fe[5\text{-}NO_2\text{-}sal\text{-}N(1,4,7,10)]$,[16,17] where $5\text{-}NO_2\text{-}sal\text{-}N(1,4,7,10)$ is a hexadentate ligand arising from the Schiff base condensation of $5\text{-}NO_2$-salicylaldehyde with 1,4,7,10-tetraazadecane; a similar plateau was found to form on warming the LS isomer (resulting from a rather fast cooling of the HS isomer) of the complex $[FeL(CN)_2]\cdot H_2O$, L being a Schiff-base ligand derived from the condensation of 2,6-diacetylpyridine with 3,6-dioxaoctane-1,8-diamine;[18] finally, quite recently, the variable-temperature magnetic susceptibility, far infrared and $^{57}Fe$ Mössbauer data obtained for $Fe(4,4'\text{-}dpb)_2(NCS)_2$, where 4,4'-dpb stands for 4,4'-diphenyl-2,2'-bipyridine, were interpreted as being indicative of a two-step spin transition involving the iron(II) spin states $S = 2$, $S = 1$, and $S = 0$.[19] Two theoretical approaches were proposed to account for such a spin-crossover peculiarity.[20,21] Both are based on the presumed existence of two nonequivalent sites for the molecules in the lattice unit cell. However, for Zelentsov et al.,[20] the existence of two steps results from both the difference between the ground level energy gaps in the two sites and the one

(1) (a) Universitat de València. (b) Laboratoire de Chimie Inorganique Université Paris-Sud. (c) Université Pierre et Marie Curie. (d) Laboratorie de Chimie Physique des Matériaux Amorphes, Université Paris-Sud.
(2) Gütlich, P. *Struct. Bonding (Berlin)* **1981**, *44*, 83.
(3) König, E.; Ritter, G.; Kulshreshtha, S. K. *Chem. Rev.* **1985**, *85*, 219.
(4) Rao, C. N. R. *Int. Rev. Phys. Chem.* **1985**, *4*, 19.
(5) Toftlund, H. *Coord. Chem. Rev.* **1989**, *94*, 67.
(6) Ivanov, E. V. Thesis, Institute of Technical Physics, Moscow, USSR, 1969.
(7) Zelentsov, V. V. *Sov. Sci. Rev. B. Chem.* **1987**, *10*, 485.
(8) Köppen, H.; Müller, E. W.; Köhler, C. P.; Spiering, H.; Meissner, E.; Gütlich, P. *Chem. Phys. Lett.* **1982**, *91*, 348.
(9) Meissner, E.; Köppen, H.; Spiering, H.; Gütlich, P. *Chem. Phys. Lett.* **1983**, *95*, 163.
(10) Meissner, E. Ph.D. Thesis, Department of Physics, University of Mainz, Germany, 1984.
(11) Köppen, H. Ph.D. Thesis, Department of Chemistry, University of Mainz, Germany, 1985.
(12) Kaji, K.; Sorai, M. *Thermochim. Acta* **1985**, *88*, 185.
(13) Wiehl, L.; Kiel, G.; Köhler, C. P.; Spiering, H.; Gütlich, P. *Inorg. Chem.* **1986**, *25*, 1565.
(14) Gütlich, P.; Hauser, A. *Coord. Chem. Rev.* **1990**, *97*, 1.
(15) Köhler, C. P.; Jakobi, R.; Meissner, E.; Wiehl, L.; Spiering, H.; Gütlich, P. *J. Phys. Chem. Solids* **1990**, *51*, 239.
(16) Petrouleas, V.; Tuchagues, J. P. *Chem. Phys. Lett.* **1987**, *137*, 21.
(17) Rakotonandrasana, A.; Boinnard, D.; Savariault, J. M.; Tuchagues, J. P.; Petrouleas, V.; Cartier, C.; Verdaguer, M. *Inorg. Chim. Acta* **1991**, *180*, 19.
(18) König, E.; Ritter, G.; Dengler, J.; Nelson, S. M. *Inorg. Chem.* **1987**, *26*, 3582.
(19) Figg, D. C.; Herber, R. H.; Felner, I. *Inorg. Chem.* **1991**, *30*, 2535.
(20) Zelentsov, V. V.; Lapouchkin, G. I.; Sobolev, S. S.; Shipilov, V. I. *Dokl. Akad. Nauk.* **1986**, *289*, 393.

0002-7863/92/1514-4650$03.00/0 

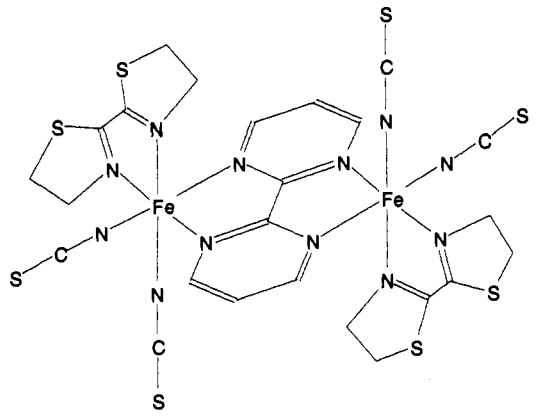

**Figure 1.** Schematic drawing of the molecule of $[Fe(bt)(NCS)_2]_2bpym$.

between the interactions involving sites of similar and different types, while, for Sasaki and Kambara,[21] the phenomenon arises from the differences between the interactions of the local distortions with the lattice.

At this stage, it must be emphasized that all the compounds above-mentioned as presenting a two-step spin conversion are mononuclear species.

On the other hand, it should be noted that some polynuclear compounds are known to present a spin-crossover behavior: several iron(III) homodinuclear complexes of the type $[(FeL)_2bge](BF_4)_2$, where bge is a bridging ligand and L the pentadentate phenolic dianion of the Schiff base bis(3-salicylideneaminopropyl)amine;[22] the homodinuclear iron(II) and nickel(II) compounds $[Fe(bzp)(NCS)_2]_2bpym$ (where bzp = bromazepan and bpym = 2,2′-bipyrimidine)[23] and $[(C_5H_5)Ni\{P(S)R_2\}_2Ni(C_5H_5)]$ with R = $OCH_3$ and R = $CH_3$;[24] the two heterodinuclear species complying with the formula $[(C_5H_5)_2Mo(\mu\text{-}SBu^t)_2Ni(C_5H_4R)]BF_4$, where R = H and R = Me;[25] two linear homotrinuclear complexes, in which only the central metal ion, cobalt(III)[26-30] or iron(II),[31] exhibits the spin conversion; the iron(II) two-dimensional compound $[Fe(4,4'\text{-bis-}1,2,4\text{-triazole})_2]\cdot H_2O$;[32] the clusters $Nb_6I_{11}$ and $HNb_6I_{11}$.[33]

In all these polynuclear complexes, the spin-crossover process was found to occur in one step.

In this paper we report on the first two-step spin transition presented by a polynuclear system, namely the dinuclear iron(II) compound $[Fe(bt)(NCS)_2]_2bpym$ formed with 2,2′-bi-2-thiazoline (bt), thiocyanate groups, and 2,2′-bipyrimidine. The IR spectrum of this compound clearly shows (vide infra) that 2-2′-bipyrimidine acts as a bridging ligand, that the two $NCS^-$ groups bound to each iron(II) ion are in cis position, and that the molecules are likely to be centrosymmetrical. So, in the absence of crystals suitable to perform an X-ray diffraction structure, it is not unreasonable to represent this compound, at the molecular scale (see Figure 1), by analogy with the homologous species $[Fe(bpym)(NCS)_2]_2bpym$, the structure of which is known.[23] We present an investigation of $[Fe(bt)(NCS)_2]_2bpym$, carried out on the basis of variable-temperature magnetic susceptibility and $^{57}Fe$ Mössbauer spectrometry measurements, and differential scanning calorimetry (DSC) experiments. A theoretical model is proposed to account for the experimental data.

## Experimental Section

**Synthesis and Characterization.** The synthesis of $[Fe(bt)(NCS)_2]_2bpym$ was carried under an argon atmosphere, using deoxygenated solvents. The procedure was as follows. A 0.633-mmol sample of $Fe(py)_4(NCS)_2$ (py = pyridine) was dissolved in 30 mL of methanol at 60 °C, and a solution of bt (0.633 mmol) in dichloromethane (10 mL) was added dropwise. A deep violet solution formed. The addition of 0.316 mmol of bpym dissolved in 10 mL of methanol changed the color of this solution to deep red. The crystalline black product which formed after the mixture was refluxed for half an hour was filtered off and dried under an argon stream (yield: 55%). $Fe(py)_4(NCS)_2$ and bt were prepared according to the methods described by Erickson and Sutin[34a] and Nelson et al.[34b], respectively. It should be noted that, in the solid state, the complex is not oxygen sensitive: the α-diimine moiety of both ligands is actually known to stabilize the lower oxidation state (II) of iron. Anal. Calcd for $[Fe(bt)(NCS)_2]_2bpym$, viz., $C_{24}H_{22}N_{12}S_8Fe_2$: C, 34.05; H, 2.60; N, 19.86; S, 30.27. Found: C, 34.58; H, 2.74; N, 19.80; S. 29.15.

From IR and X-ray data, the compound was clearly shown not to be a mixture including species such as $Fe(bt)_2(NCS)_2$, $[Fe(bpym)(NCS)_2]_2bpym$, and/or $Fe(py)_4(NCS)_2$. Concerning the IR spectrum, the presence of only one strong absorption (with shoulders) between 1650 and 1700 $cm^{-1}$ indicates unambiguously that bipyrimidine occupies a bridging position (when it acts as a bidentate ligand, two intense and well-resolved absorptions are observed[23,35]); moreover, the splitting of the strong band pointing around 2060–2080 $cm^{-1}$ into two components of comparable intensity shows that the $NCS^-$ groups bound to each iron atom are in cis position; finally, the relative simplicity of the absorption pattern, in spite of the vibrational complexity of the ligands, is likely to account for a molecular centrosymmetry.

**Magnetic Susceptibility Measurements.** The variable-temperature magnetic susceptibility measurements were carried out using a Faraday-type magnetometer equipped with an Oxford Instrument helium continuous-flow cryostat and a home-made automatic data-acquisition equipment. Temperature was varied at the rate of 1 K $min^{-1}$ in the cooling as well as in the heating mode. The independence of susceptibility with regard to the applied magnetic field was checked at room temperature. $HgCo(NCS)_4$ was used as a susceptibility standard. The diamagnetic correction was estimated as $-432 \times 10^{-6}$ $cm^3$ $mol^{-1}$.

**Mössbauer Spectra.** The Mössbauer spectra were obtained on a constant-acceleration spectrometer with a 25-mCi source of $^{57}Co$ in rhodium matrix. The calibration was made with a metallic iron foil at room temperature. The experimental line width was typically 0.22 mm $s^{-1}$. The absorber was a sample of 63 mg of $[Fe(bt)(NCS)_2]_2bpym$ polycrystalline powder, enclosed in a capsule ≈1 cm in diameter, the size of which had been determined in order to get an optimum absorption. Temperature was varied in the 295–4.2 K range using a bath cryostat (Oxford MD-3), the thermal scanning being monitored by a servocontrol device (accuracy: ±0.1 K). The typical counting time was ca. 6 h. A least-squares computer program[36] was used to fit the Mössbauer parameters and to determine their standard deviations of statistical origin (given in parentheses).

**Calorimetric Measurements.** The differential scanning calorimetry experiments were performed on a Perkin-Elmer DSC-2 instrument, the low-temperature attachment of which was a home-made cooling system allowing the temperature to be lowered to 83 K.[37] Sealed sample pans were used. Both cooling and heating curves were recorded and analyzed with a TADS-3600 Perkin-Elmer system. Temperature and enthalpy were calibrated by using the melting and crystal-to-crystal transitions of a pure cyclohexane sample (279.69 K, 2678 J $mol^{-1}$ and 186.10 K, 6740 J $mol^{-1}$, respectively). The temperature values are known with a ±0.5 K accuracy, and the experimental uncertainty on the enthalpy values is ±2% for a scan rate of 10 K $min^{-1}$.

(21) Sasaki, N.; Kambara, T. *Phys. Rev. B* **1989**, *40*, 2442.
(22) Ohta, S.; Yoshimura, C.; Matsumoto, N.; Okawa, H.; Ohyoshi, A. *Bull. Chem. Soc. Jpn.* **1986**, *59*, 155.
(23) Real, J.-A.; Zarembowitch, J.; Kahn, O.; Solans, X. *Inorg. Chem.* **1987**, *26*, 2939.
(24) Klâui, W.; Schmidt, K.; Bockmann, A.; Hofmann, P.; Schmidt, H. R.; Stauffert, P. *J. Organomet. Chem.* **1985**, *286*, 407.
(25) Werner, H.; Ulrich, B.; Schubert, U.; Hofmann, P.; Zimmer-Gasser, B. *J. Organomet. Chem.* **1985**, *297*, 27.
(26) Klâui, W. *J. Chem. Soc., Chem. Commun.* **1979**, 700.
(27) Gütlich, P.; McGarvey, B.; Klâui, W. *Inorg. Chem.* **1980**, *19*, 3704.
(28) Eberspach, E.; El Murr, N.; Klâui, W. *Angew. Chem., Int. Ed. Engl.* **1982**, *21*, 915.
(29) Navon, G.; Klâui, W. *Inorg. Chem.* **1984**, *23*, 2722.
(30) Klâui, W.; Eberspach, W.; Gütlich, P. *Inorg. Chem.* **1987**, *26*, 3977.
(31) Vos, G.; le Fêbre, R. A.; de Graaff, R. A. G.; Haasnoot, J. G.; Reedijk, J. *J. Am. Chem. Soc.* **1983**, *105*, 1682.
(32) Vreugdenhil, W.; van Diemen, J. H.; de Graaff, R. A. G.; Haasnoot, J. G.; Reedijk, J.; van der Kraan, A. M.; Kahn, O.; Zarembowitch, J. *Polyhedron* **1990**, *24*, 2971.
(33) Imoto, H.; Simon, A. *Inorg. Chem.* **1982**, *21*, 308.
(34) (a) Erickson, N. E.; Sutin, N. *Inorg. Chem.* **1966**, *5*, 1834. (b) Nelson, J.; Nelson, S. M.; Perry, W. D. *J. Chem. Soc., Dalton Trans.* **1976**, 1282.
(35) (a) Castro, I.; Julve, M.; De Munno, G.; Bruno, G.; Real, J.-A.; Lloret, F.; Faus, J. *J. Chem. Soc., Dalton Trans.*, in press. (b) De Munno, G.; Julve, M.; Verdaguer, M.; Real, J.-A., submitted to *Inorg. Chem.*
(36) Varret, F. *Proceedings of the International Conference on Mössbauer Effect Applications*; Jaipur, 1981.
(37) Dworkin, A.; Jaffrê, J.; Szwarc, H. *Rev. Scient. Instrum.* **1991**, *62*, 1654.

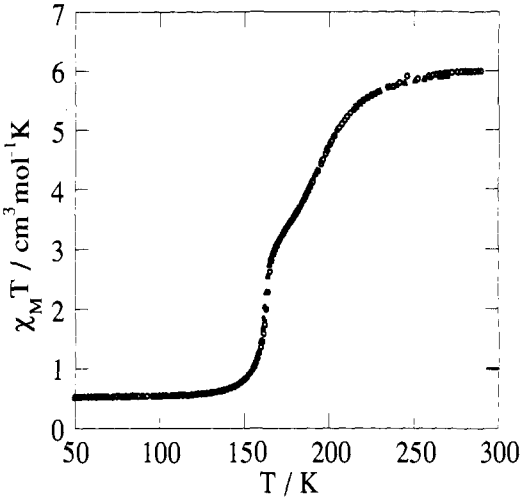


**Figure 2.** Temperature dependence of $\chi_M T$ for $[Fe(bt)(NCS)_2]_2bpym$, in the cooling (○) and heating (△) modes.

## Results

**Magnetic Susceptibility Data.** The variable-temperature magnetic susceptibility data obtained for $[Fe(bt)(NCS)_2]_2bpym$ in the range ca. 295–50 K provide evidence for an overall $S = 2 \leftrightarrow S = 0$ spin-crossover behavior. At room temperature, the $\chi_M T$ product ($\chi_M$ being the molar magnetic susceptibility and $T$ the temperature) is 5.98 cm$^3$ mol$^{-1}$ K, which corresponds to an effective magnetic moment $\mu_{eff} = 6.92\ \mu_B$ and shows that most of the iron(II) ions are in the HS state. The proportion of metal ions which are then retained in the LS state was found to be ≈9% from Mössbauer data (vide infra). It follows that the $\chi_M T$ value relative to the pure HS species can be estimated as 6.57 cm$^3$ mol$^{-1}$ K ($\mu_{eff} = 7.25\ \mu_B$). This value lies in the range expected for an iron(II) dinuclear complex including two noncoupled or weakly coupled HS metal ions. At 50 K, $\chi_M T = 0.53$ cm$^3$ mol$^{-1}$ K ($\mu_{eff} = 2.06\ \mu_B$), which is characteristic of LS iron(II) ions with a residual amount (≈8%) of HS ones. The spin-change phenomenon does not present a noticeable thermal hysteresis, for the curves $\chi_M T$ vs $T$ resulting from measurements performed at decreasing and increasing temperatures are indistinguishable, as seen in Figure 2.

These curves clearly reveal that the spin crossover takes place in two steps. The so-called "step 1" and "step 2" are centered around the temperatures 163 and 197 K, respectively. The former is rather abrupt, 80% of the spin change occurring within ca. 15 K; the latter is smoother. Between ≈169 and ≈181 K the spin conversion is more gradual than below and above this temperature range. At the intermediate inflexion point, around 175 K, the $\chi_M T$ value is ca. 3.35 cm$^3$ mol$^{-1}$ K, which corresponds to a HS iron(II) fraction of ≈51%.

These magnetic susceptibility data do not allow us to determine the magnitude of the magnetic interaction between the two HS iron(II) ions of a molecule of $[Fe(bt)(NCS)_2]_2bpym$. However, by analogy with the results reported for three other compounds of the type $[FeL(NCS)_2]_2bpym$ (where L are the bidentate ligands 2,2′-bipyridine, 2,2′-bipyrimidine, or bromazepan),[23] the pairwise exchange interaction is expected to be antiferromagnetic, with a $J$ parameter in the range −4 to −5 cm$^{-1}$ (defining $J$ from the hamiltonian $\mathcal{H} = -J(\hat{S}_A \cdot \hat{S}_B)$, where $\hat{S}_A$ and $\hat{S}_B$ are the local spin operators).

**Thermodynamic Parameters.** A typical example of the calorimetric results is given in Figure 3. The curve represented was recorded at increasing temperatures and is indicative of an endothermic process. The existence of two peaks separated by an interval of ca. 30 K, viz., a sharp one with a maximum at 164 K and a broad one with a maximum at 194 K, is in agreement with the data resulting from magnetic susceptibility measurements and, as will be seen hereafter, from Mössbauer spectrometry.

The onsets of the two steps of the transition are found at ≈157 and ≈172 K in the heating mode and ≈163 and ≈206 K in the cooling mode. The discrepancy observed between these values and those deduced from the magnetic measurements (i.e., ≈ 163 and ≈197 K) may be accounted for by the fact that the temperature scan rate chosen for the calorimetric experiments was relatively high (10 K min$^{-1}$)—this condition being necessary for a satisfying accuracy on the value of the overall enthalpy variation $\Delta H$ to be obtained—, by the closeness of the two peaks in the temperature scale and by the broadness of the high-temperature peak.

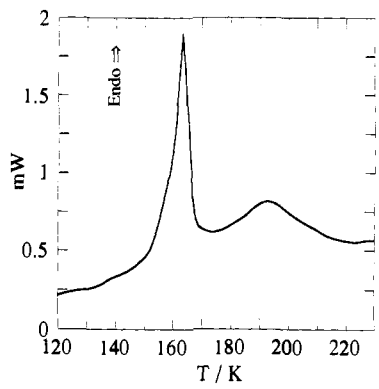


**Figure 3.** DSC curves obtained for $[Fe(bt)(NCS)_2]_2bpym$ in the heating mode, at a scan rate of 10 K min$^{-1}$.

The average $\Delta H$ value, deduced from a number of experiments performed at increasing and decreasing temperatures, is found equal to 13.3 ± 0.5 kJ mol$^{-1}$ after correction for the presence of LS iron(II) ions at room temperature and HS ones at low temperature. The components of $\Delta H$ corresponding to the temperature ranges below and above 175 K, i.e., to HS iron(II) fractions lower and higher than ≈50%, respectively, can then be evaluated as $\Delta H_1 = 7.9 \pm 0.5$ kJ mol$^{-1}$ and $\Delta H_2 = 5.4 \pm 0.5$ kJ mol$^{-1}$.

The overall entropy variation upon the stepwise spin transition, calculated with $\int (C_p/T)dT$ from the $C_p$ vs $T$ diagram ($C_p$ being the molar heat capacity), is $\Delta S = 82 \pm 6$ J K$^{-1}$ mol$^{-1}$, which corresponds to 41 ± 3 J K$^{-1}$ mol$^{-1}$ per iron unit. This latter value is somewhat lower than the values reported for a number of mononuclear iron(II) complexes exhibiting a first-order spin transition (i.e., 48–65 J K$^{-1}$ mol$^{-1}$)[38-44] but is very close to that recently found for $Fe(py)_2(phen)(NCS)_2$ (with phen = 1,10-phenanthroline), i.e., 37 J K$^{-1}$ mol$^{-1}$.[45] As expected, it is significantly larger than the entropy variation resulting from the change in spin state alone, viz., $\Delta S_{spin} = R \ln [(2S+1)_{HS}/(2S+1)_{LS}] = 13.4$ J K$^{-1}$ mol$^{-1}$. It is well-known that the excess can be mostly attributed to the vibrational contribution ($\Delta S_{vib} \approx 28$ J K$^{-1}$ mol$^{-1}$), which mainly arises from the change in the stretching and deformation modes of the coordination core.

**Mössbauer Spectrometry Data.** Some representative Mössbauer spectra of $[Fe(bt)(NCS)_2]_2bpym$ obtained in the heating mode are shown in Figure 4. The low-temperature and high-temperature main doublets are typical for the low-spin and high-spin states of iron(II), respectively: isomer shift (IS) values are 0.411 (1) mm s$^{-1}$ at 4.5 K and 0.995 (1) mm s$^{-1}$ at 270 K; quadrupole splitting ($\Delta E_q$) values are in agreement with the data reported for iron(II) spin-crossover complexes.[2,4] At intermediate temperatures, both contributions are clearly resolved, which indicates the coexistence of LS and HS iron(II) ions; the presence of narrow lines shows that the LS ↔ HS conversion rates are slow compared to the hyperfine frequencies (ca. $10^8$ s$^{-1}$), except above 240 K,

(38) Sorai, M.; Seki, S. *J. Phys. Chem. Solids* **1974**, *35*, 555.
(39) Hoselton, M. A.; Wilson, L. J.; Drago, R. S. *J. Am. Chem. Soc.* **1975**, *97*, 1722.
(40) Katz, B. A.; Strouse, C. E. *J. Am. Chem. Soc.* **1979**, *101*, 6214.
(41) Kulshreshtha, S. K.; Iyer, R. M. *Chem. Phys. Lett.* **1984**, *108*, 501.
(42) Kaji, K.; Sorai, M. *Thermochim. Acta* **1985**, *88*, 185.
(43) Kulshreshtha, S. K.; Sasikala, R. *Chem. Phys. Lett.* **1986**, *123*, 215.
(44) Kulshreshtha, S. K.; Iyer, R. M. *Chem. Phys. Lett.* **1987**, *134*, 239.
(45) Claude, R.; Real, J.-A.; Zarembowitch, J.; Kahn, O.; Ouahab, L.; Grandjean, D.; Boukheddaden, K.; Varret, F.; Dworkin, A. *Inorg. Chem.* **1990**, *29*, 4442.

**Table I.** Least-Squares Fitted Mössbauer Data[a,b]

| | low-spin state | | | high-spin state | | | |
|---|---|---|---|---|---|---|---|
| $T$ (K) | IS (mm s$^{-1}$) | $\Delta E_q^{HS}$ (mm s$^{-1}$) | $\Gamma$ (mm s$^{-1}$) | IS (mm s$^{-1}$) | $\Delta E_q^{LS}$ (mm s$^{-1}$) | $\Gamma$ (mm s$^{-1}$) | $A_{HS}/A_{tot}$ (%) |
| 4.5 | 0.411 (1) | 0.466 (1) | 0.286 (2) | 1.27 | 3.1 | 0.34 | 3 |
| 78 | 0.406 (1) | 0.459 (1) | 0.258 (2) | 1.27 (3) | 2.62 (5) | 0.58 (8) | 5 |
| 170 | 0.383 (1) | 0.482 (2) | 0.264 (2) | 1.056 (2) | 2.797 (4) | 0.284 (6) | 34 |
| 190 | 0.388 (2) | 0.452 (2) | 0.278 (6) | 1.041 (1) | 2.842 (3) | 0.330 (5) | 65 |
| 270 | 0.11 (3) | 0.57 (4) | 0.50 (6) | 0.995 (1) | 2.598 (3) | 0.280 (4) | 85 |

[a] IS = monomer shift, $\Delta E_q$ = quadrupole splitting, $\Gamma$ = half-height width of the lines, $A_{HS}/A_{tot}$ = area ratio. [b] With their statistical standard deviations given in brackets; underlined values were fixed for the fit; isomer shift values refer to metallic iron at 300 K. $A$ = base-line-corrected area.

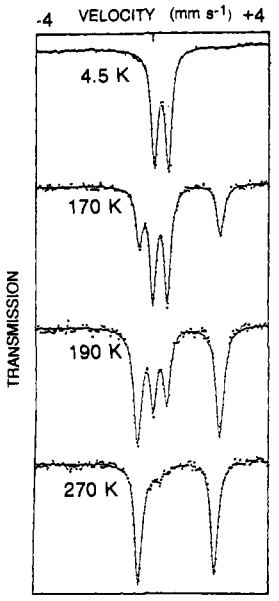


**Figure 4.** Selected Mössbauer spectra of [Fe(bt)(NCS)$_2$]$_2$bpym, obtained in the heating mode.

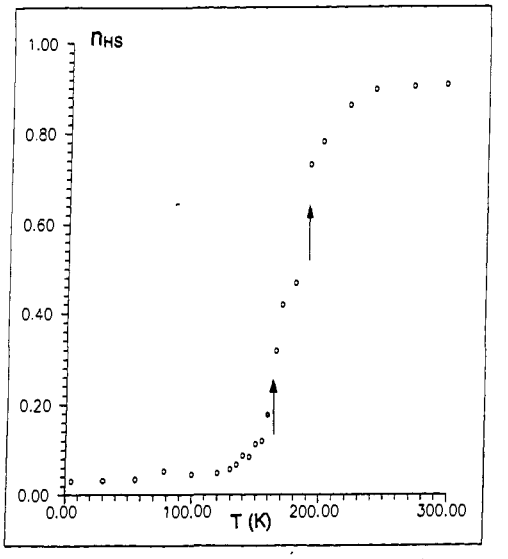


**Figure 5.** Thermal variation of $n_{HS}$ deduced from the ratio of the Mössbauer absorption areas, corrected for Lamb–Mössbauer factors. The arrows point at the steepest parts of the curve and hence depict the macroscopic steps of the transition.

where the line broadening of the "low-spin doublet" indicates that the conversion rates are approaching this limit.[46,47] Least-squares fitted data are reported in Table I.

The thermal dependence of the area ratio $A_{HS}/A_{tot}$ clearly shows the two steps of the transition. However, the actual value of the HS iron(II) fraction slightly differs from this ratio, through the Lamb–Mössbauer factors $f_{HS}(T)$, $f_{LS}(T)$, as shown by the relation

$$n_{HS}/n_{LS} = (A_{HS}/A_{LS}) \times (f_{LS}/f_{HS})$$

The values of $f_{LS,HS}(T)$ have been deduced from an analysis of the thermal dependence of the total area in the Debye approximation (Debye temperatures: $\Theta_D$(HS) = 134 (2) K, $\Theta_D$(LS) = 156 (2) K), including a thickness correction by a simple formula.[48,49] The variation of $n_{HS}$ as a function of temperature is shown in Figure 5. This curve compares with the $\chi_M T$ vs $T$ plot (cf. Figure 2): two steps are again observed for the transition, step 1 being steeper than step 2; they are centered around 162 and 189 K, as indicated by the arrows in the figure. The low-temperature residual HS fraction is found to be ca. 4%, i.e., somewhat lower than that deduced from the magnetic data, viz., 8%. This is likely to result from the fact that experiments were performed with samples arising from several preparations, which is well-known to possibly lead to some difference in particle sizes and hence in the development of the spin conversion, in particular at low temperature. Moreover, evidence is provided for the existence of ca. 9% of LS iron(II) ions at room temperature. In the *plateau* between step 1 and step 2 the $n_{HS}$ ratio is again found to be close to 50%.

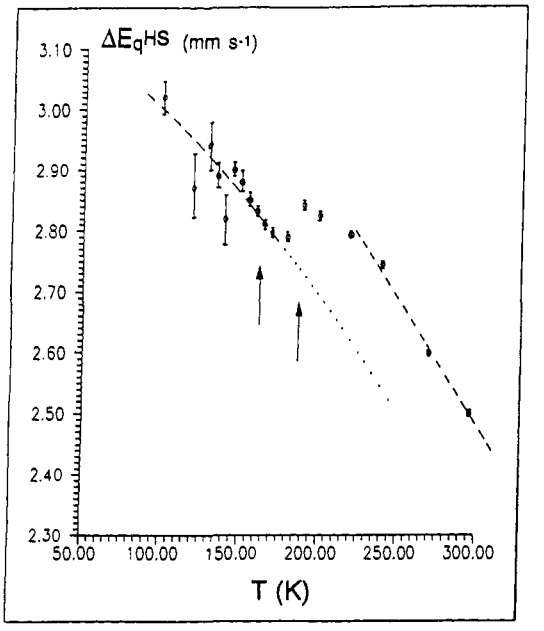


**Figure 6.** Thermal variation of the quadrupole splitting of the high-spin doublet. The dotted line is a likely extrapolation of the low-temperature curve, which corresponds to the LS,HS (SQ) molecules. The arrows have the same meaning as in Figure 5.

The thermal variation of the quadrupole splittings was carefully analyzed.

(i) The high-spin quadrupole splitting (see the curve $\Delta E_q^{HS}$ vs $T$ in Figure 6) is a sensitive probe for molecular rearrangements, due to the orbital properties of the $^5T_{2g}$ electronic state.

(46) Adler, P.; Hauser, A.; Vef, A.; Spiering, H.; Gütlich, P. *Hyperfine Interact.* **1989**, *47*, 343.
(47) Adler, P.; Spiering, H.; Gütlich, P. *J. Chem. Phys.* **1989**, *50*, 587.
(48) Henry, M.; Teillet, J.; Varret, F. *Rev. Phys. Appl.* **1980**, *15*, 1095.
(49) Boukheddaden, K.; Varret, F. *Hyperfine Interact.*, in press.

First of all, it clearly appears that the sample is not a mixture of two one-step transition structural phases. In such a case, these phases should undergo a similar jump in $\Delta E_q^{HS}$, but at different temperatures, and the Mössbauer spectra, in the *plateau*, should contain two well-resolved doublets. The observation of only one doublet confirms that the sample is made of a single structural phase exhibiting a two-step transition.

Secondly, the large $\Delta E_q^{HS}$ values indicate a local symmetry lower than cubic, with a rather well isolated ground orbital singlet. The thermal variation of $\Delta E_q^{HS}$ exhibits a jump around 180 K and presents quasi linear portions on both sides of the jump. In the high-temperature branch, the slope $d\Delta E_q/dT$ can be accurately determined by linear regression and is evaluated as $-3.8 \times 10^{-3}$ mm s$^{-1}$ K$^{-1}$. A similar behavior was reported for HS iron(II) ions in $K_2ZnF_4$ matrix,[50] with a comparable slope, viz., $-2.82 \times 10^{-3}$ mm s$^{-1}$ K$^{-1}$; the data were analyzed in a full vibronic treatment and led to $\delta = 590$ cm$^{-1}$, $\delta$ being the strength of the low-symmetry ligand field. Arguing that the slope should roughly vary as $\delta^{-1}$ we deduce that, in the present case, $\delta \approx 450$ cm$^{-1}$ in the high-temperature branch (assuming similar vibrational properties). The jump in $\Delta E_q^{HS}$ is not satisfactorily explained by a simple change in $\delta$ (an increase in $\delta$ should result in both an increase in $\Delta E_q^{HS}$ and a decrease in the slope); we therefore suspect that it mainly originates from a change in vibrational properties.

The most striking feature of Figure 6 is that the variation of $\Delta E_q^{HS}$ as a function of temperature ignores step 1 but detects step 2. This can be explained in the frame of the two-step intramolecular model developed in the next section. The "macroscopic" steps detected by magnetic, Mössbauer, and calorimetric measurements essentially reflect the "microscopic" two steps of the intramolecular spin conversion

$$\text{LS,LS} \overset{1}{\leftrightarrow} \text{LS,HS} \overset{2}{\leftrightarrow} \text{HS,HS}$$

or

$$\text{SS} \leftrightarrow \text{SQ} \leftrightarrow \text{QQ}$$

using the notations of the theoretical approach (vide infra), where S stands for spin singlet and Q for spin quintet.

The fact that step 1 is not detected means that $\Delta E_q^{HS}$ is not sensitive to intermolecular effects (the Mössbauer probe belongs to a molecule which has already passed through step 1, and the occurrence of step 1 on the neighboring molecules is an intermolecular event). The variation detected at step 2, when the second iron atom of the same molecule converts from the LS to the HS state, shows that $\Delta E_q^{HS}$ is, as expected, sensitive to intramolecular effects.

(ii) The low-spin quadrupole splitting, due to the isotropic properties of the $^1A_{1g}$ electronic state, is less sensitive to intramolecular changes. The present data are consistent with the simple assumption that $\Delta E_q^{LS}$ is only sensitive to intermolecular effects, through the "lattice" contribution. Indeed, the temperature dependence of $\Delta E_q^{LS}$ plotted in Figure 7, which on the one hand is nearly the same below ≈160 and above ≈180 K and on the other hand reflects both steps of the transition with almost opposite effects, can be interpreted as follows: the similar thermal behavior of $\Delta E_q^{LS}$ on both sides of the transition range would result from the fact that the HS and LS phases have the same space group, which is expected to lead to the same value of the "lattice" term, i.e., to the same $\Delta E_q^{LS}(T)$ values (it should be noted that, in most cases, the space group of the spin-crossover systems was found to be retained upon the transition);[51,52] in the temperature range between step 1 and step 2, the relatively high concentration of the LS,HS (SQ) species would modify the crystal structure, which might explain the large change in the $\Delta E_q^{LS}$ values.

An additional observation supports the picture of an intramolecular two-step transition: the variations in $\Delta E_q$ values (for both high- and low-spin states) are four times larger than those

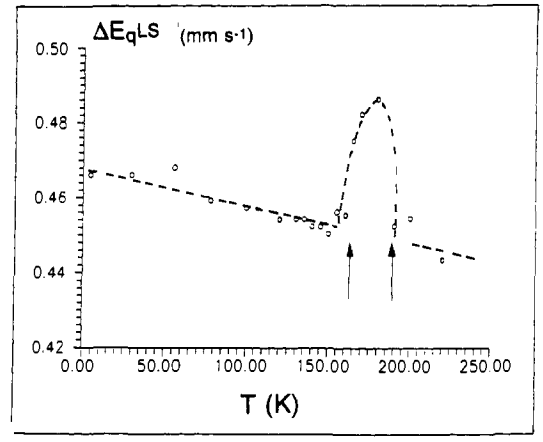


**Figure 7.** Thermal variation of the quadrupole splitting of the low-spin doublet. The arrows have the same meaning as in Figure 5.

observed for the two-step transitions presented by mononuclear complexes.[8,16] This suggests that the LS ↔ HS conversions detected through the $\Delta E_q$ changes occur in the close vicinity of the Mössbauer probe. Within this picture, the existence of narrow "high-spin lines" upon step 2 requires the LS,HS ↔ HS,HS conversion rates to be fast enough to average the corresponding contributions (these rates should be faster than the difference in the corresponding hyperfine frequencies, i.e., ca. $10^7$ s$^{-1}$).

## Theoretical Approach

In this section we propose a model accounting for a two-step transition in iron(II) dinuclear species. The two iron(II) ions, noted A and B, can undergo a S ↔ Q spin transition between singlet (S) and quintet (Q) spin states. Within the dinuclear molecule the two metal ions may be in the singlet state (SS), in the quintet state (QQ), or one in the singlet state and the other one in the quintet state (SQ). The total enthalpy and entropy variations accompanying the transformation SS → QQ are noted $\Delta H$ ($= H_{QQ} - H_{SS}$) and $\Delta S$ ($= S_{QQ} - S_{SS}$), respectively. We assume that the molecule has an inversion center relating the two metal ions and that the site symmetry of the Fe(II) ion is low enough in order for the orbital degeneracy of the Q state to be removed. If so, SS gives rise to a unique pair state $^1\Gamma_g$, SQ to two pair states $^5\Gamma_g + {}^5\Gamma_u$, and QQ to five pair states $^1\Gamma_g + {}^3\Gamma_u + {}^5\Gamma_g + {}^7\Gamma_u + {}^9\Gamma_g$. The symbols $\Gamma_g$ and $\Gamma_u$ stand for gerade and ungerade irreducible representations of the group describing the symmetry properties of the dinuclear molecule.

The energy differences between the states arising from QQ are only due to the intramolecular magnetic interaction. As mentioned above, the interaction between two high-spin iron(II) ions through the 2,2′-bipyrimidine bridge is known to be weak. This effect may be assumed not to be crucial and will not be considered anymore. If so, the states associated with QQ are degenerate with an enthalpy $\Delta H$, the enthalpy origin being the enthalpy of SS.

The two states arising from SQ are supposed to be degenerate as well with an energy $\Delta H/2 + W$ where $W$ is a small positive or negative correction with regard to $\Delta H/2$. For $W \neq 0$, the energy of the SQ states is not rigorously halfway between those of the SS and QQ states. The SQ situation is slightly favored or disfavored according to whether $W$ is negative or positive, respectively.

Let us give now some information on the origin of W. There are two contributions, one of electrostatic, the other one of vibronic origin. The former contribution accounts for the fact that the electronic repulsion $R_{SQ}$ between the two iron(II) ions in the SQ states is not exactly equal to half of the sum of the electronic repulsions in the SS and QQ states $(R_{SS} + R_{QQ})/2$. This can be easily shown as follows. The d-type orbitals are noted $a_i$ ($i = 1$–5) around A, and $b_j$ ($j = 1$–5) around B. The orbitals $a_1$, $a_2$, $a_3$, $b_1$, $b_2$, and $b_3$ arise from the $t_{2g}$ subsets, and $a_4$, $a_5$, $b_4$, and $b_5$ from the $e_g$ subsets. Furthermore, $a_1$ (or $b_1$) is the d-type orbital of lowest energy. Since the orbital degeneracy in the Q state is assumed to be totally removed, the electronic configurations in

(50) Ducouret-Cêrêze, A.; Varret, F. *J. Phys. (Paris)* **1988**, *49*, 661.
(51) König, E. *Progr. Inorg. Chem.* **1987**, *35*, 527.
(52) Gallois, B.; Real, J.-A.; Hauw, C.; Zarembowitch, J. *Inorg. Chem.* **1990**, *29*, 1152.

the local S and Q states are as follows:

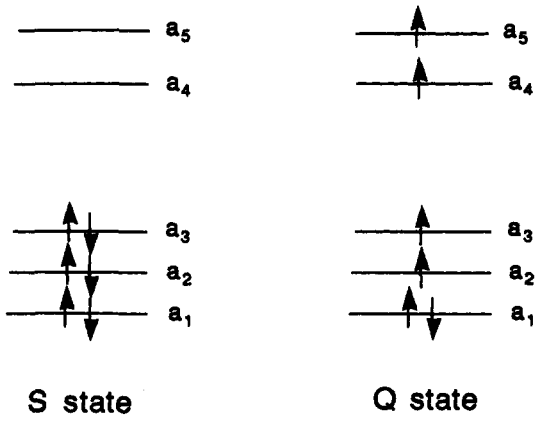


Ignoring the indiscernability of the electrons, i.e., neglecting the two-electron exchange integrals as compared to the two-electron coulomb integrals results in the electrostatic repulsions

$$R_{SS} = 4\sum_{i=1}^{3}\sum_{j=1}^{3} j_{ij} \quad (1)$$

$$R_{SQ} = 4\sum_{i=1}^{3} j_{i1} + 2\sum_{i=1}^{3}\sum_{j=2}^{5} j_{ij} \quad (2)$$

$$R_{QQ} = 4j_{11} + 4\sum_{j=2}^{5} j_{1j} + \sum_{i=2}^{5}\sum_{j=2}^{5} j_{ij} \quad (3)$$

with

$$j_{ij} = \left\langle a_i(1)b_j(2)\left|\frac{1}{r_{12}}\right|a_i(1)b_j(2)\right\rangle \quad (4)$$

and $j_{ij} = j_{ji}$ owing to the symmetry of the dinuclear molecule. Equations 1–3 verify that

$$R_{SQ} \neq (R_{SS} + R_{QQ})/2 \quad (5)$$

The latter contribution, of vibronic nature, is more difficult to introduce. A full treatment will appear elsewhere. We restrict ourselves to say here that taking into account the breathing vibrations of the iron(II) coordination sphere results in a $W_{vib}$ contribution defined by

$$W_{vib} = k_S k_Q (q_S - q_Q)^2/2(k_S + k_Q) \quad (6)$$

$k_S$ and $k_Q$ being the force constants, and $q_S$ and $q_Q$ the equilibrium values of the internal coordinate $q$ involved in the potential energy eqs 7 and 8 for the local S and Q states

$$E_S = E_S^0 + (k_S/2)(q - q_S)^2 \quad (7)$$

$$E_Q = E_Q^0 + (k_Q/2)(q - q_Q)^2 \quad (8)$$

Equation 6 is valid only when the dinuclear molecule is assumed to be centrosymmetrical even in the SQ states. This may happen through coupling of the A(S)–B(Q) and A(Q)–B(S) mixed-spin states.

What precedes is summed up in the diagram below

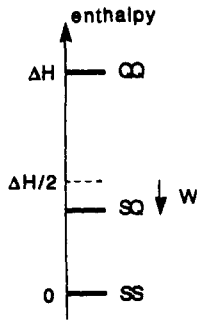


where the energy shift $W$ of the SQ states may be negative or positive. In the following we will use the parameter $\rho = 2W/\Delta H$.

The process we are interested with may be schematized as

$$\underset{x}{SS} \leftrightarrow \underset{y}{SQ} \leftrightarrow \underset{z}{QQ} \quad (9)$$

where $x$, $y$, and $z$ are the molar fractions of each of the spin isomers, with

$$x + y + z = 1 \quad (10)$$

The Gibbs free energy of the system at the temperature $T$ is

$$G = xG_{SS} + yG_{SQ} + zG_{QQ} + \Gamma(x,y,z) - TS_{mix} \quad (11)$$

$G_{SS}$, $G_{SQ}$, and $G_{QQ}$ are the molar Gibbs free energies of the SS, SQ, and QQ pure phases, respectively. $S_{mix}$ is the mixing entropy

$$S_{mix} = k(N \ln N - Nx \ln Nx - Ny \ln Ny - Nz \ln Nz) \quad (12)$$

where $k$ is the Boltzmann constant and $N$ the Avogadro number. $S_{mix}$ may be rewritten as

$$S_{mix} = -R(x \ln x + y \ln y + z \ln z) \quad (13)$$

$R = Nk$ being the perfect gas constant. The excess Gibbs energy $\Gamma(x,y,z)$ accounts for intermolecular interactions at the scale of the lattice. A general expression for this term in the quasichemical approach[53] is

$$\Gamma = \gamma(xy + \alpha yz + \beta zx) \quad (14)$$

so that $\gamma$ is the interaction parameter between SS and SQ molecules, $\alpha\gamma$ between SQ and QQ molecules, and $\beta\gamma$ between SS and QQ molecules. A simplification consists in assuming that only the interactions between S and Q iron(II) ions belonging to two different dinuclear molecules occur in $\Gamma(x,y,z)$. If so, $\alpha$ is equal to 1 and $\beta$ to 2. This simplification is in line with Slichter and Drickamer's model[54] valid for mononuclear species, in which the interaction term is proportional to the product of the molar fractions of S and Q molecules. The expression for $G$ becomes

$$\begin{aligned} G &= xG_{SS} + yG_{SQ} + zG_{QQ} + \\ &\quad \gamma(xy + yz + 2zx) + RT(x \ln x + y \ln y + z \ln z) \\ &= y(\Delta H/2 + W) + z\Delta H + \gamma(xy + yz + 2zx) - \\ &\quad T[(y/2 + z)\Delta S - R(x \ln x + y \ln y + z \ln z)] \end{aligned} \quad (15)$$

where the state SS is taken as both the enthalpy and entropy origin. In (15), it is assumed that both entropy variations $S_{QQ} - S_{SQ}$ and $S_{SQ} - S_{SS}$ are equal to $\Delta S/2$. This point will be discussed further in the next section. The equilibrium conditions for the process (9) are given by

$$\left(\frac{\partial G(x,y)}{\partial x}\right)_T = 0 \quad \text{and} \quad \left(\frac{\partial G(x,y)}{\partial y}\right)_T = 0 \quad (16)$$

the condition (10) remaining valid. The two equations in eq 16 have no analytical solution, and the problem has been solved by looking for the minima of $G$ at various temperatures, which leads to the $x = f(T)$, $y = f(T)$, and hence $z = f(T)$ curves. The results may also be expressed in the form of $c = f(T)$ curve, $c$ being the molar fraction of iron(II) ions in the Q state, related to $y$ and $z$ through

$$c = (y + 2z)/2 \quad (17)$$

The molar fraction $c$ slightly differs from $n_{HS}$ introduced above. Indeed our model does not account for the incompleteness of the transition both at very low and high temperatures. So, $c$ results from the normalization of $n_{HS}$ in order to tend to zero when $T$ approaches the absolute zero and to a value very close to 1 when $T$ becomes large. Let us define now the critical temperature $T_c$ as the temperature for which $c$ is equal to 0.5. Using the Lagrange

(53) Swalin, R. A. *Thermodynamics of Solids*; John Wiley and Sons, Inc.: New York, London, Sydney, 1967; p 109.
(54) Slichter, C. P.; Drickamer, H. G. *J. Chem. Phys.* **1972**, *56*, 2142.

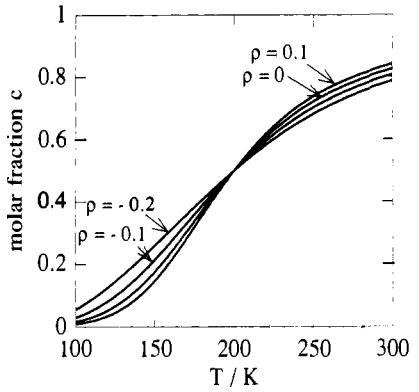


**Figure 8.** High-spin molar fraction $c$ versus $T$ curves for $\Delta H$ = 1000 cm$^{-1}$, $\Delta S$ = 5 cm$^{-1}$ K$^{-1}$, $\gamma$ = 0, and $\rho$ = 0.1, 0, −0.1, and −0.2. One recalls that $\rho$ is defined as $2W/\Delta H$.

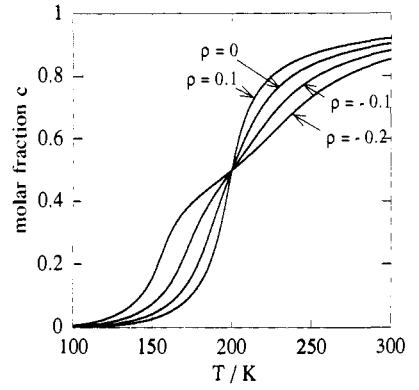


**Figure 9.** High-spin molar fraction $c$ versus $T$ curves for $\Delta H$ = 1000 cm$^{-1}$, $\Delta S$ = 5 cm$^{-1}$ K$^{-1}$, $\gamma$ = 166 cm$^{-1}$, and $\rho$ = 0.1, 0, −0.1, and −0.2.

multipliers technique, the minimum of $G(x,y,z)$ may be found through

$$\frac{\partial}{\partial x}\left[G(x,y,z) + \Lambda(x + y + z)\right] = 0 \qquad (18)$$

$$\frac{\partial}{\partial z}\left[G(x,y,z) + \Lambda(x + y + z)\right] = 0 \qquad (19)$$

Equation 18 leads to

$$\gamma(y + 2z) + RT(\ln x + 1) + \Lambda = 0 \qquad (20)$$

and (19) leads to

$$\Delta H - T\Delta S + \gamma(y + 2x) + RT(\ln z + 1) + \Lambda = 0 \qquad (21)$$

At $T = T_c$, $x = z$, so that comparing (20) and (21) results in

$$T_c = \Delta H/\Delta S \qquad (22)$$

We see that $T_c$ is related to enthalpy and entropy variations through the same equation as the one valid for mononuclear species. In particular, $T_c$ does not depend on $W$.

Before focusing on the magnetic and thermodynamical behaviors of the title compound, we would like to discuss the results arising from our model in a more general fashion. For that, we first define a critical value $\gamma_c$ of the intermolecular interaction parameter; $\gamma_c$ is the $\gamma$ value above which the $G(x,y,z)$ function presents more than a single minimum in a given temperature range for $W = 0$. This definition is a straightforward extension of the definition of $\gamma_C$ for mononuclear spin-transition molecules in Slichter and Drickamer's model; $\gamma_c$ is then equal to $2R\Delta H/\Delta S$, and for $\gamma > \gamma_c$ a thermal hysteresis is thermodynamically possible. In the case of dinuclear molecules, $\gamma_c$ is found larger than $2R\Delta H/\Delta S$. For instance, for $\Delta H$ = 1000 cm$^{-1}$ and $\Delta S$ = 5 cm$^{-1}$ K$^{-1}$, $\gamma_c$ is equal to 332 cm$^{-1}$, whereas $2R\Delta H/\Delta S$ is equal to 278 cm$^{-1}$.

In a second step, we have quantitatively investigated the role of $\rho = 2W/\Delta H$ for three different values of $\gamma$, namely 0, 166, and

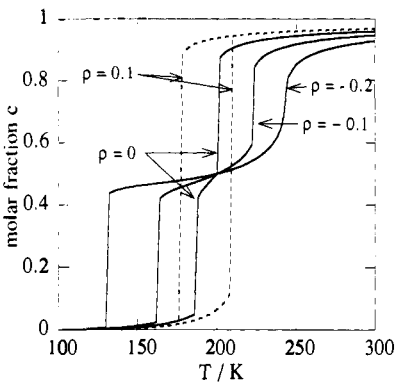


**Figure 10.** High-spin molar fraction $c$ versus $T$ curves for $\Delta H$ = 1000 cm$^{-1}$, $\Delta S$ = 5 cm$^{-1}$ K$^{-1}$, $\gamma$ = 332 cm$^{-1}$, and $\rho$ = 0.1, 0, −0.1, and −0.2.

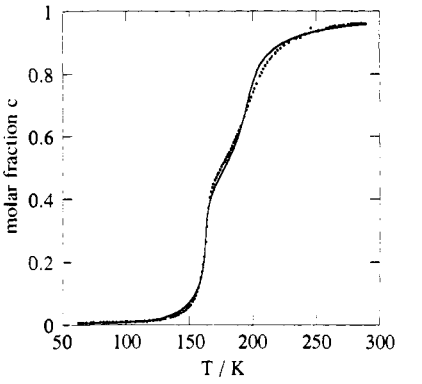


**Figure 11.** Experimental and calculated temperature dependences of the high-spin molar fraction $c$ (see text).

332 cm$^{-1}$, $\Delta H$ remaining equal to 1000 cm$^{-1}$, and $\Delta S$ to 5 cm$^{-1}$ K$^{-1}$. Figure 8 shows the $c = f(T)$ curves for $\gamma$ = 0 and $\rho$ = +0.1, 0, −0.1, and −0.2. The transition in any case is very gradual, but decreasing $\rho$ down to negative values results in even smoother transitions. For $\rho < 0$, actually, the transition is more gradual than expected for a Boltzmann equilibrium between ground S and excited Q states. Figure 9 shows the same curves for $\gamma$ = 166 cm$^{-1}$, i.e., $\gamma_c/2$. Again we observed that a negative $\rho$ value makes the transition more gradual. For $\rho$ = −0.2, the very beginning of a two-step transition appears. Figure 10 corresponds to $\gamma = \gamma_c$ = 332 cm$^{-1}$. For $\rho$ = 0, a two-step transition is observed. A positive $\rho$ value not only suppresses the two-step character but also gives a thermal hysteresis with abrupt transitions both in the cooling and warming modes. On the other hand, the more negative $\rho$, the more pronounced the two-step character is. It is also worth remarking that the low-temperature step is always more abrupt than the high-temperature one. When $\gamma$ is larger than $\gamma_c$, the solutions of eq 16 become very tedious to find, and we did not explore further the mathematical problem. We already have enough information to understand the origin of the two-step transitions in dinuclear compounds; they result from a synergistic effect between a negative $\rho$ value and a large $\gamma$ value. Those two parameters are related to interactions between iron(II) ions, the former within the dinuclear molecule, the latter between the molecules. When $\gamma$ is large enough, a two-step transition may be observed for $\rho$ = 0; the phenomenon, however, is the more pronounced as $\rho$ becomes more negative. When $\gamma$ is small, a very negative $\rho$ value is required in order for the phenomenon to be observed.

Let us now consider the $c$ versus $T$ curve deduced from the experimental magnetic data of Figure 2. An excellent agreement shown in Figure 11 between calculated and experimental $c = f(T)$ curves is obtained for $\Delta H$ = 1100 cm$^{-1}$ (13.16 kJ mol$^{-1}$), $\Delta S$ = 6.16 cm$^{-1}$ K$^{-1}$ (73.7 J K$^{-1}$ mol$^{-1}$), $\gamma$ = 215 cm$^{-1}$ (2.57 kJ mol$^{-1}$), and $W$ = −40 cm$^{-1}$ (−478 J mol$^{-1}$). $\rho$ is then equal to −0.072. The critical temperature defined as $\Delta H/\Delta S$ is equal to 178.6 K. At $T_c$ the molar fractions of SS, SQ, and QQ species are $x_c = z_c$ = 0.15, and $y_c$ = 0.70.

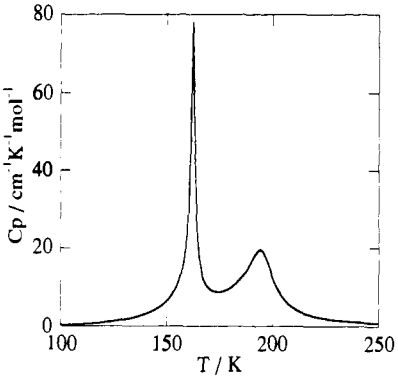


**Figure 12.** Simulation of the heat capacity curve with the enthalpy parameters deduced from the fitting of the magnetic data.

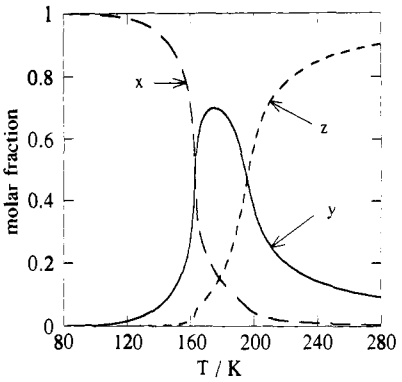


**Figure 13.** Molar fractions of SS ($x$), SQ ($y$), and QQ ($z$) species versus $T$ plots deduced from the fitting of the magnetic data.

Our model accounts for the magnetic properties of [Fe(bt)-(NCS)$_2$]$_2$bpym in a quantitative fashion. We want to show now that it accounts for the calorimetric behavior as well. In particular, it reproduces the main features of the experimental data, i.e., the presence of two peaks, one rather sharp with a high maximum below $T_c$, the other one much broader with a weaker maximum above $T_c$. The enthalpy $H(T)$ at the temperature $T$ may be written as

$$H(T) = y(\Delta H/2 + W) + z\Delta H + \gamma(xy + yz + 2zx) \quad (23)$$

with $H(0) = 0$. The heat capacity $C_p(T)$ may then be calculated as $\partial H(T)/\partial T$. Using the $\Delta H$, $W$, and $\gamma$ values given above results in the curve of Figure 12 showing the two asymmetrical peaks above and below $T_c$. It is also possible to calculate $\Delta H_1$ and $\Delta H_2$ defined as

$$\Delta H_1 = H(T_c) - H(0)$$

$$\Delta H_2 = H(T \rightarrow \infty) - H(T_c) \quad (24)$$

$H(T_c)$ is given by

$$H(T_c) = \Delta H/2 + (1 - 2z_c)W + 2z_c\gamma(1 - z_c) \quad (25)$$

the enthalpy of SS being again taken as the enthalpy origin, which leads to

$$\Delta H_1 = \Delta H/2 + (1 - 2z_c)W + 2z_c\gamma(1 - z_c) \quad (26)$$

$$\Delta H_2 = \Delta H/2 - (1 - 2z_c)W - 2z_c\gamma(1 - z_c) \quad (27)$$

In eqs 25–27, it is assumed that the interaction Gibbs free energy $\Gamma(x,y,z)$ is entirely of enthalpy origin. Introducing the numerical values of $\Delta H$ $W$, $\gamma$, and $z_c$ given above in eqs 26 and 27 results in $\Delta H_1 = 577$ cm$^{-1}$ (6.90 kJ mol$^{-1}$) and $\Delta H_2 = 523$ cm$^{-1}$ (6.26 kJ mol$^{-1}$). The experimental values are 7.9 ± 0.5 and 5.4 ± 0.5 kJ mol$^{-1}$.

## Discussion and Conclusion

Even if some cases of two-step spin transition have already been reported, the situation encountered in [Fe(bt)(NCS)$_2$]$_2$bpym is quite novel. Indeed, the two-step character is intimately related to the dinuclear nature of the compound. The Mössbauer spectra clearly confirm that the observed behavior does not result from the presence of two one-step transition polymorphs; the sample contains a unique phase exhibiting a two-step transition. A model has been developed to account for this peculiarity. Its cornerstone is that the enthalpy of the SQ species in which an iron(II) ion is in the S local state and the other in the Q local state may not be exactly halfway between the enthalpies of the SS and QQ like-spin species [$H_{SQ} \neq (H_{SS} + H_{QQ})/2$]. A two-step transition may be expected when $H_{SQ}$ is lower than $(H_{SS} + H_{QQ})/2$. This condition, however, may not be sufficient; in addition, a significant cooperativity within the crystal lattice is required. It follows that the two-step character arises from the synergistic effect between intramolecular interactions favoring the SQ states and intermolecular interactions favoring the formation of like-species domains.

Another way to describe the situation is to say that the SQ species is favored with respect to what the statistics would predict for a randomly distributed mixture of iron(II) ions in S and Q states, with $1 - c$ and $c$ molar fractions, respectively. In such a system, the probability to find SS pairs is $x = (1 - c)^2$, SQ pairs $y = 2c(1 - c)$, and QQ pairs $z = c^2$. It turns out that at $T_c$ we have $x = z = 0.25$ and $y = 0.50$. These statistical values have to be compared to what has been found for [Fe(bt)(NCS)$_2$]$_2$bpym, namely $x = z = 0.15$ and $y = 0.70$. The temperature dependences of $x$, $y$, and $z$ as determined in our calculation are shown in Figure 13.

As far as the origin of the stabilization of SQ is concerned, we already mentioned that two mechanisms might be invoked, one of electrostatic, the other one of vibronic origin. This problem will be treated in a thorough manner in a subsequent paper. It seems to us sufficient to point out here that $H_{SQ}$ has no reason to be strictly equal to $(H_{SS} + H_{QQ})/2$. The enthalpy deviation $W$ we found is only a small fraction (7.2%) of the enthalpy gap $(H_{SS} + H_{QQ})/2$. It is enough to give rise to the two-step transition.

In the calculation, it has been assumed that the five QQ states, on the one hand, and the two SQ states, on the other hand, were accidentally degenerate or, more exactly, that the magnetic interaction energy was negligible as compared to $W$. The comparison of the value found for $W$ with the overall splitting $10J$ of the QQ states does not fully justify our assumption. It is likely more correct to define $\Delta H$ as the barycenter of the QQ states and, similarly, $\Delta H/2 + W$ as the barycenter of the SQ states. However, neglecting the small splittings of the QQ and SQ states is not crucial in the model. Without this assumption, two additional energy parameters characterizing these splittings would be involved so that the model would likely be overparametrized. Along the same line, the assumption that the entropy differences $S_{QQ}$–$S_{SQ}$ and $S_{SQ}$–$S_{SS}$ are equal is not crucial either; it makes the model simpler. We also supposed that the mixed-spin species retained the inversion center. This may happen if the electronic coupling between A(S)–B(Q) and A(Q)–B(S) is large enough. The problem of the symmetry of those mixed-spin species is quite interesting in itself, but not directly related to the appearence of a two-step transition. Our model remains valid if the SQ species are not centrosymmetrical anymore. Only eq 6 has then to be modified.

What we attempted to do in this work is to build the simplest model accounting for two-step spin transitions in dinuclear compounds. Our model emphasizes the key role of intramolecular $W$ and intermolecular $\gamma$ interaction parameters. It seems to us quite remarkable that in spite of its rusticity this model reproduces not only the magnetic behavior with the low-temperature step more abrupt than the high-temperature one but also the heat capacity curve. As a matter of fact, it has been possible to simulate the heat capacity curve from the energy parameters $\Delta H$, $W$, and $\gamma$ deduced from the fitting of the $\chi_M T$ versus plot. The calculated heat capacity curve shows the main features of the experimental one, in particular the rather sharp peak below $T_c$, and the smoother and less intense peak above $T_c$. Furthermore, the calculated values of the enthalpy variations below and above $T_c$ compare fairly well with the experimental ones. It is worth mentioning here that the uncertainty on the values $\Delta H_1$ and $\Delta H_2$ deduced from the DSC measurements is rather large.

Perhaps, the weakest point of our approach concerns the term $\Gamma(x,y,z)$ accounting for intermolecular interactions. The expression of $\Gamma(x,y,z)$ in (6) implicitly supposes that the SS, SQ, and QQ species are statistically distributed, whereas the cooperativity should favor the formation of like-species domains. The larger the interaction parameter $\gamma$, the more pronounced this defect is. Actually, this deficiency is present in the original Slichter and Drickamer's model from which we drew inspiration.

To conclude, we want to point out that it is not quite correct to attribute the step 1, below $T_c$, to the SS $\leftrightarrow$ SQ process, and the step 2, above $T_c$, to the SQ $\leftrightarrow$ QQ process. Each step involves SS, SQ, and QQ species, even if the proportions of QQ in step 1 and SS in step 2 are weak. According to our calculation (see Figure 13), $z$ is equal to 0.043 at 163 K, and $y$ is equal to 0.051 at 197 K.

The long term goal of our work dealing with polynuclear species incorporating spin-transition ions is to tune the shape of the signal provided by the $\chi_M T$ versus $T$ plot.[55] This would be required to control both the intra- and intermolecular interactions. Molecular and crystal engineerings are involved in such a project, together with theoretical studies.

(55) Zarembowitch, J.; Kahn, O. *New J. Chem.* **1991**, *15*, 181.

# Control over the Relative Stereochemistry at C4 and C5 of 4,5-Dihydrooxepins through the Cope Rearrangement of 2,3-Divinyl Epoxides and a Conformational Analysis of This Ring System

**Whe-Narn Chou,[†] James B. White,*[,†] and William B. Smith*[,‡,1]**

*Contribution from the Department of Chemistry, Box 19065, The University of Texas at Arlington, Arlington, Texas 76019, and the Chemistry Department, Box 32908, Texas Christian University, Fort Worth, Texas 76129.* *Received June 24, 1991*

**Abstract:** The Cope rearrangement of *cis*-2,3-divinyl epoxides was used to control the relative stereochemistry at C4 and C5 of 4,5-dihydrooxepins. Wadsworth–Horner–Emmons olefination of either (4*E*)-*cis*-2,3-epoxy-5-(trimethylsilyl)-4-pentenal (**3**) or (5*E*)-*cis*-3,4-epoxy-6-(trimethylsilyl)-5-hexen-2-one (**4**) provided the cis epoxides used in this study. The termini of their 1,5-dienes were thereby substituted at one end with a trimethylsilyl group with fixed *E* stereochemistry and at the other with either a carboalkoxy or cyano substituent as both the *Z* and *E* isomers. The rearrangements were carried out within a temperature range of 95–135 °C, and all of the rearrangements were stereospecific, each leading to a single 4,5-dihydrooxepin. Based on a presumed boatlike transition state for these rearrangements, the (1*E*,5*E*)-*cis*-3,4-epoxy-1,5-hexadienes **5a–e** led to the *cis*-4,5-dihydrooxepins **7a–e**, and the (1*E*,5*Z*)-*cis*-3,4-epoxy-1,5-hexadienes **6a,c–e** led to the *trans*-4,5-dihydrooxepins **8a,c–e**. In general, those 1,5-dienes containing a *Z* double bond rearranged slower than the corresponding *E* isomers. A solvent affect was found in the [3,3] sigmatropic rearrangement of substrates containing *Z*-$\alpha,\beta$-unsaturated esters, $CH_3CN$ being a more effective solvent than $CCl_4$. It was further found that *Z*-$\alpha,\beta$-unsaturated nitiriles rearranged more cleanly than the corresponding esters. The relative stereochemistry at C4 and C5 can greatly affect the subsequent reactivity of the oxepin nucleus, as illustrated by the greater kinetic acidity of the cis isomer of 4-carbomethoxy-5-(trimethylsilyl)-4,5-dihydrooxepin (**7a**) compared to that of its trans isomer **8a**. The ester of the former compound was easily deprotonated at −70 °C in THF by $LiN(TMS)_2$ and the resultant enolate alkylated at the $\alpha$ carbon by MeI, conditions that led to the complete recovery of the trans isomer. These results are consistent with the assignment of cis and trans stereochemistry of these oxepins. From their $^1H$ NMR spectra, all of the *trans*-4,5-dihydrooxepins appeared to be similar to each other in terms of their coupling patterns and constants, but the *cis*-4,5-dihydrooxepins could be divided up into two groups on the basis of their coupling constants. For three of the oxepins, *cis*-4,5-dihydrooxepins **7a** and **7c** and *trans*-4,5-dihydrooxepin **8a**, the assignment of their coupling patterns was confirmed by 2-D NMR. The minimum-energy conformations of these three oxepins were determined by molecular mechanics calculations. The conformational preferences were explicable in terms of two steric interactions: allylic $A^{1,2}$ strain and the gauche interaction at C4 and C5.

## Introduction

Aranotin acetate (**1**) is a fungal metabolite exhibiting antiviral activity and containing two 4,5-dihydrooxepin nuclei that are identical both in their functionality and in their absolute stereochemistry.[2] One possible retrosynthetic analysis of this molecule, involving a disconnection of the epidithiapiperazinedione moiety, leads to the advanced intermediate **2**, which could also be used as an intermediate for a number of other structurally related fungal metabolites.[3] One of the problems inherent in the synthesis of

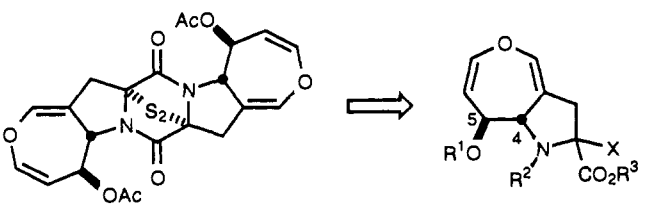


1 aranotin acetate 2 X=H or $SR^4$

**2** is the control of the relative stereochemistry at C4 and C5 of the 4,5-dihydrooxepin ring. The preparation of 4,5-dihydrooxepins

[†] The University of Texas at Arlington.
[‡] Texas Christian University.

0002-7863/92/1514-4658$03.00/0 